

Computational Study of Mixed Heat Convection in Annular Space between Concentric Rotating Inner and Wavy Surface Outer Cylinders

Qusay Rasheed Al-Amir*, Farooq Hassan Ali Alinnawi and Qusay Adnan

Department of Mechanical Engineering, Faculty of Engineering, University of Babylon, Babylon Province, Al Hillah, Babylon City, Iraq

ABSTRACT

Mixed heat convection inside annular spaces occurs in many engineering technology applications. This study aims to determine the effect of the sinusoidal surface parameters of an outer cylinder, which are represented by variations in the undulation number and amplitude of the wavy surface, on flow structure and thermal fields for different values of the Reynolds number (Re ; from 0 to 600) and Rayleigh number (Ra ; from 10^3 to 10^6). A horizontal annular space bounded by two concentric cylinders contained air with a Prandtl number that equaled 0.7. The sinusoidal surface of the fixed circular outer cylinder was maintained at a constant cold temperature (T_c), whereas the surface of the circular inner cylinder was set at a constant hot temperature (T_h) and rotated in counter-clockwise direction at constant angular velocity. Calculations were performed under steady-state conditions. A computational procedure based on the finite volume technique was implemented using the software ANSYS Fluent (version 16.1). Results indicate that the heat transfer from the inner cylinder increased with a rise in the surface amplitudes and undulation numbers with a fixed

Re . The average Nusselt number increased with an increase in Ra and reduced when the undulation number increased from one to two. In summary, the heat transfer of the cylinder with the sinusoidal outer surface is better by 7.3% than that of the conventional cylinder.

Keywords: Annular space, concentric cylinders, mixed convection, rotating cylinder, surface amplitude, undulation number

ARTICLE INFO

Article history:

Received: 11 March 2018

Accepted: 23 April 2019

Published: 21 October 2019

E-mail addresses:

qusay1972@gmail.com (Qusay Rasheed Al-Amir)

farooq_hassan77@yahoo.com (Farooq Hassan Ali Alinnawi)

qam_me782000@yahoo.com (Qusay Adnan)

* Corresponding author

INTRODUCTION

Mixed convection heat transfer within annular spaces has been a topic of interest for decades. The mixed convection problem in finite spaces is present in several industrial and environmental applications, including the ventilation of buildings, waste transport and storage of nuclear and chemical reactors, design of electronic equipment (Mozayyeni & Rahimi, 2011), cooling systems (Yoo, 1998), different types of solar collectors and thermal storage systems (Bande & Mariah, 2014) and thermal management in aviation (Xu et al., 2009). Moreover, mixed convection is becoming increasingly important in engineering applications, especially because enclosures with internal bodies are more complicated than classical enclosures. Mixed convection in different enclosure geometries, such as square, rectangle and cylinder, has been investigated in various studies (Shih et al., 2009; Chamkha et al., 2011; Hussain & Abd-Amer, 2011; Wang et al., 2015; Rajamohan et al., 2015). These studies experimentally, analytically and numerically investigated mixed convection in annular spaces under different boundary conditions.

Sheikholeslami et al. (2012) developed a FEM model of the natural convection heat transfer in an annular space bounded by a circular outer enclosure and a sinusoidal circular inner cylinder. Their study was conducted at different dimensionless groups, such as the Hartmann number (Ha), Rayleigh number (Ra), volume fraction of nanoparticles and undulation number of the inner cylinder. The authors revealed that the (\overline{Nu}) variation was a function that increased with the volume fraction of nanoparticles, the number of undulations and Ra but decreased with Ha . Sheikholeslami et al. (2013) studied the effect of the amplitude and the undulation number of a hot sinusoidal inner cylinder on the natural convection problem with the assumption that the enclosure (circular outer) was filled with air and maintained at a cold temperature. Their works covered a wide range of parameters ($Ra = 10^3, 10^4, 10^5$ and 10^6), amplitudes ($L = 0.1, 0.3$ and 0.5) and numbers of undulations of the inner cylinder ($N = 2, 3, 5$ and 6). These authors found that the flow and temperature patterns and cells (number, size and formation) strongly depended on the Ra , undulation number and amplitude of the enclosure. Magneto hydrodynamic flow in a nanofluid-filled inclined enclosure was numerically investigated by Sheikholeslami et al. (2014), who concluded that the velocity field retarded and the convection and Nusselt number (Nu) decreased in the existence of the magnetic field. Shekar et al. (1984) numerically studied the convective heat transfer and flow characteristics of a fluid filling the space between two horizontal concentric cylinders. The results were obtained under the effects of an externally imposed temperature gradient across the annulus and uniform internal heat generation. The authors concluded that the ratio of the characteristic temperature had an important role in the flow behaviour, in which the flow fields comprised one or two vortices in each half cavity. Xu et al. (2010) conducted laminar natural convective heat transfer around a horizontal cylinder inside a concentric triangular enclosure. The researchers concluded

that the predicted overall Nu of an inclination angle was independent of the inclination angle. Laminar natural heat transfer around a coaxial triangular inner cylinder to its concentric cylindrical enclosure was performed by Yu et al. (2010). The results revealed that the temperature distribution became nearly independent of the Prandtl number. Yuan et al. (2015) analysed the free convection in the horizontal concentric annuli problem with different inner cylinders. They concluded that the surface radiation and presence of corners and large top space played an important role in enhancing the heat transfer rate.

The mixed convection in the entry region of a vertical annulus with a rotating inner cylinder was presented by El-Shaarawi and Sarhan (1982). Their results indicated that the hydrodynamic development length and heat transfer parameters were affected by the rotating inner cylinder. Yoo (1998) investigated numerically the mixed convection heat transfer characteristics of air within two horizontal concentric cylinders with different uniform temperatures. Their investigation revealed the flow regimes on the Ra–Re plane, and they presented and explained the characteristics of the velocity patterns and the heat transfer. Mohammed (2007) used a numerical finite difference method to obtain the solution to the mixed convection in the entry region of a vertical annulus containing an inner cylinder. The results showed that the thickness of the thermal boundary layer gradually increased as the flow moved from the annulus inlet towards the annulus exit. Alam et al. (2016) studied mixed convection inside a differentially heated square enclosure containing a rotating heat conducting cylinder. The results indicated that the flow field, temperature distribution and rate of heat transfer were dependent on cylinder size and rotating speeds. Alsabery et al. (2018) studied the effect of rotating solid cylinder on entropy generation and convective heat transfer in a wavy porous cavity heated from below. They showed that the heat transfer rate from the wall to the fluid increased with the Darcy number and, in particular, increased significantly for $Da > 10^{-3}$.

A few experimental studies on the natural convective heat transfer across an annulus with a hexagonal inner cylinder and a concentric circular outer cylinder have been conducted, such as that by Boyd (1984). A correlation for the mean Nu at the surface of the inner cylinder was presented for a specific range of Ra and expressed as $Nu = 0.794 Ra^{0.25}$. The results revealed that the presence of hexagonal inner element corners enhanced the average Nu compared with the heat transfer in a circular inner cylinder. Lee (1992) conducted an experimental and numerical study on the effect of the convective fluid motion of air enclosed between the annuli of inner and eccentric horizontal cylinders, which were assumed to be heated and rotating. The influence of the cylinder through its rotating speed on the resulting convection problem was investigated. The result showed that the higher the rotational Re, the more the flow tended to become uniform. Furthermore, the inner rotational cylinder remarkably affected the mean Nu. Another experimental work was presented by Rajamohan et al. (2015) to explore the effect of various inclination angles on

the mixed convection heat transfer of a thermally developing flow in a side-heated square duct. The authors found that an increase in the inclination angle improved the convection rate and hence remarkably enhanced the heat transfer.

As previously mentioned in the literature, mixed convection in annular spaces bounded with one corrugated surface has not been explored. The present work aims to investigate the mixed convection heat transfer in the annular space between concentric cylinders with corrugated outer and smooth inner surfaces. The effect of various parameters, such as undulation number, amplitude of the wavy surface, Re and Ra , is considered. These parameters are investigated in a wide range to examine the isotherms and streamline contours of the annular space.

PHYSICAL MODEL AND COORDINATE SYSTEM

Figure 1 shows a schematic of the two-dimensional concentric cylinders; the outer cylinder is a sinusoidal, whereas the inner one is circular. In this study, the air is utilised as the working fluid, and the ratio between the inner diameter cylinder and the subdivision of the mean radius of the outer and inner radius cylinders ($R_i/(R_{om}-R_i)$) is equal to 2. Therefore, the characteristic length is equal to the space between the two concentric cylinders (i.e. $R_{om}-R_i$). The sinusoidal outer and circular inner cylinders are assumed to have the same centre in the origin of the Cartesian coordinate. The functions are applied to obtain the sinusoidal wavy wall on the surface of the circular cylinder.

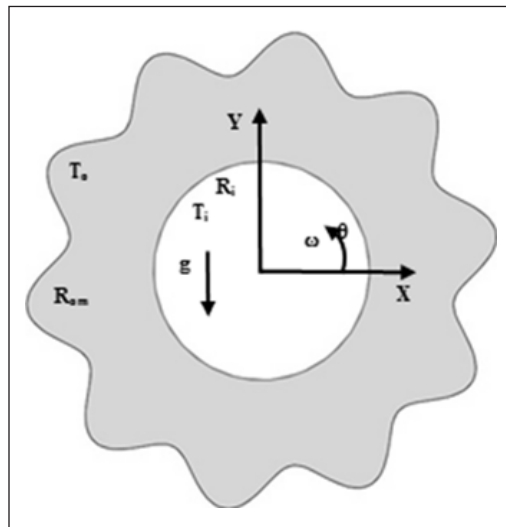


Figure 1. Physical model of the present study

$$X = [R + L \sin(n * \theta * \pi/180)/n] * \left(\cos \left(\theta * \frac{\pi}{180} \right) \right) \quad [1]$$

$$Y = [R + L \sin(n * \theta * \pi/180)/n] * \left(\sin \left(\theta * \frac{\pi}{180} \right) \right) \quad [2]$$

where X and Y are the Cartesian coordinates, R is the relaxation function, L is the amplitude of the wavy surface, n is the undulation number and θ is the angle of the circular cylinder. The cylinder length is assumed infinite where the length to diameter ratio is very long. The outer and inner cylinders are kept at cold and hot temperatures, respectively, and the difference between them is fixed at 50° . The difference in the temperature that

produces the buoyancy effect leads to natural convection, whereas the rotation of the inner cylinder with rotating velocity (ω) leads to forced convection. Hence, the combination of these conditions produces mixed convection effects.

GOVERNING EQUATIONS AND BOUNDARY CONDITIONS

In the present study, the software ANSYS Fluent version 16.1 (ANSYS, 2014) was used to solve the governing equations. The control volume technique was used to transfer the governing equation to algebraic equations. The numerical solutions were based on the control volume approach with the integration of the governing equation in each control volume and then discretization of the equations that were transferred from any quantity to the control volume. The governing continuity equation and momentum and energy equations for laminar, incompressible, two-dimensional and steady state can be written with following dimensionless variables.

$$X = \frac{x}{R_c}, Y = \frac{y}{R_c}, U = \frac{u}{u_0}, V = \frac{v}{v_0}, P = \frac{p}{\rho u_0^2}, \Phi = \frac{T - T_c}{\Delta T}, \Psi = \frac{\psi}{u_0 R_c}, Pr = \frac{\nu}{\alpha},$$

$$Re = \frac{u_0 R_c}{\nu}$$

Continuity Equation:

$$\frac{\partial U}{\partial X} + \frac{\partial V}{\partial Y} = 0 \quad [3]$$

Momentum Equations:

$$U \frac{\partial U}{\partial X} + V \frac{\partial V}{\partial Y} = -\frac{\partial P}{\partial X} + \frac{1}{Re} \left(\frac{\partial^2 U}{\partial X^2} + \frac{\partial^2 U}{\partial Y^2} \right) \quad [4]$$

$$U \frac{\partial V}{\partial X} + V \frac{\partial V}{\partial Y} = -\frac{\partial P}{\partial Y} + \frac{1}{Re} \left(\frac{\partial^2 V}{\partial X^2} + \frac{\partial^2 V}{\partial Y^2} \right) + \frac{Ra}{Pr Re^2} \Phi \quad [5]$$

Energy Equation:

$$U \frac{\partial \Phi}{\partial X} + V \frac{\partial \Phi}{\partial Y} = \frac{1}{Re Pr} \left(\frac{\partial^2 \Phi}{\partial X^2} + \frac{\partial^2 \Phi}{\partial Y^2} \right) \quad [6]$$

where ρ is the fluid density, u and v are the Cartesian velocity components, u_0 and v_0 are reference Cartesian velocity components, Ψ is dimensionless stream function, P is the dimensionless pressure, g is the gravitational acceleration, μ is dynamic viscosity, T is the temperature and α is the thermal diffusivity. In the present work, air is used as the working fluid and has a Prandtl number of 0.71. The reference temperature is set to 300 K ($T_r = \frac{T_o + T_i}{2}$). Table 1 lists the properties of air of this reference temperature. In addition, Ra is defined as

$$Ra = \frac{g \beta \Delta T R_c^3}{\nu^2} \quad [7]$$

where T_h and T_c are the hot and cold temperatures, respectively; l is the length of the annulus; ν is the kinematic viscosity and β is the thermal expansion ($\beta = \frac{1}{T_r}$), which changes with Ra. The boundary conditions are assumed as follows.

At the outer cylinder surface, $T_o = 275$ K and $u = v = 0$.

At the inner cylinder surface, $T_i = 325$ K, $u = \omega r \sin\theta$ and $v = \omega r \cos\theta$.

The local Nusselt number (Nu_s) can be calculated to estimate the heat transfer rate along the hot inner cylinder surface. It is a non-dimensional term that is defined as follows:

$$Nu_s = \frac{h \cdot ds}{k_r} \quad [8]$$

Where h is convective heat transfer coefficient ($W m^{-2} K^{-1}$), d_s is inner circular cylinder perimeter (m), and k_r is thermal conductivity $W m^{-1} K^{-1}$. In the analysis, the average Nusselt number (\overline{Nu}) is defined as

$$\overline{Nu} = \frac{1}{2\pi} \int_0^{2\pi} Nu \cdot ds \quad [9]$$

We adopted a mapped mesh, with a number of divisions equal to 140 for inner, outer cylinder (Edge sizing) and the space between them (face meshing) which produced 19740 nodes and 19600 elements to describe the heat transfer and fluid flow behaviour between the two concentric cylinders, as shown in Figure 2. A grid check with specific conditions, namely, number of corrugations = 15, amplitude (L) = 0.5, $Ra = 10^5$, $Re = 118.678$, was tested to obtain a suitable number of elements with high accuracy (i.e. continuity = 10^{-6} , $V_x = 10^{-6}$, $V_y = 10^{-6}$ and energy = 10^{-8}) (Figure 3). The convergence criteria discretization of the CFD solution was supposed for the relative error for any dependent variables satisfies the discretisation convergence criteria is $\left| \frac{\zeta_{i+1} - \zeta_i}{\zeta_{i+1}} \right| \leq \Gamma$. Where (i) signifies the number of iterations and (Γ) is the discretization convergence criteria. Many grid independent checks were examined to evaluate the grid sensitivity. Table 2 shows the grid independence check and percentage error. The error is plotted as a function of iteration number are shown in Figure 4. The value of $Re=118.678$ is corresponding to the Richardson number $Ri=10$ which represents the middle value between pure natural convection ($Ri= \infty$) and pure forced convection ($Ri=0$). The reference values for velocity (angular velocity $\omega=2.35793$ rad/s, density ($\rho=1.1614$ kg/m³), dynamic viscosity ($\mu=1.846 \cdot 10^{-5}$ m²/s). The values of Rayleigh number are $Ra=10^3$, 10^4 and 10^5 . The reference quantities for Rayleigh number are ($\alpha=2.25 \cdot 10^{-5}$ m²/s), ($\nu=1.589 \cdot 10^{-5}$ m²/s), the temperature difference $\Delta T=50$, characteristic length ($r=0.02$ m), gravitational acceleration ($g=9.81$ m/s²) and β is varied corresponding to Rayleigh number. No remarkable change occurs in the average Nu when the element number reaches 19,600.

Table 2
 Error discretization of grid independence for average Nusselt number along the hot inner cylinder for $N=15$, $L=0.5$, $Ra=10^5$, $Re=118.678$

Number of Divisions <u>Outer cylinde * Inner cylinde</u> Face meshing	Number of elements	Mean Nusselt number at the hot wall	Error (%)
40 * 40 40	1600	1.177	-
60 * 60 60	3600	1.186	0.7862
80 * 80 80	6400	1.187	0.0378
120 * 120 120	14400	1.191	0.3093
140 * 140 140	19600	1.191	0.0014

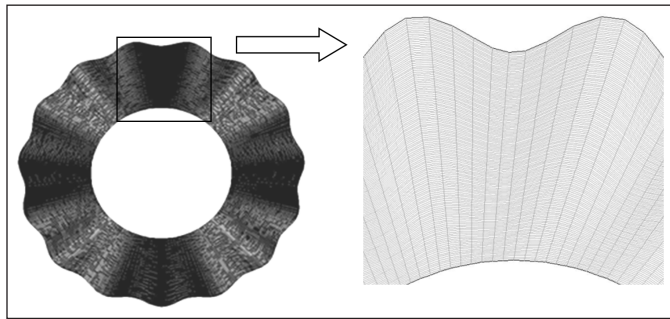


Figure 2. Mapped mesh of the present study

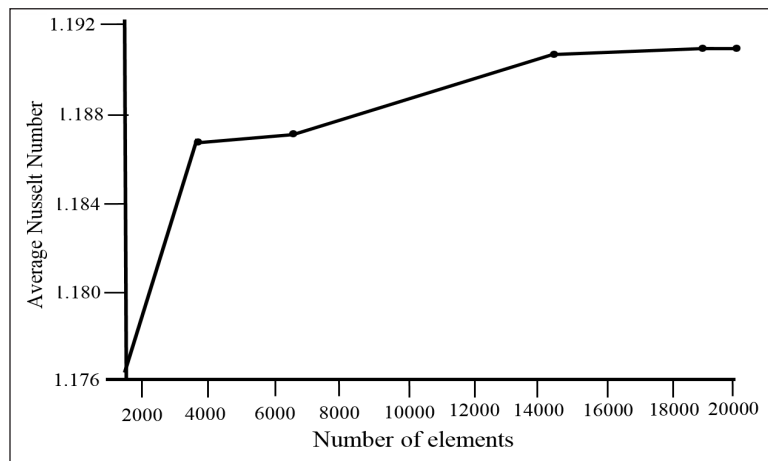


Figure 3. Verification of mesh generation

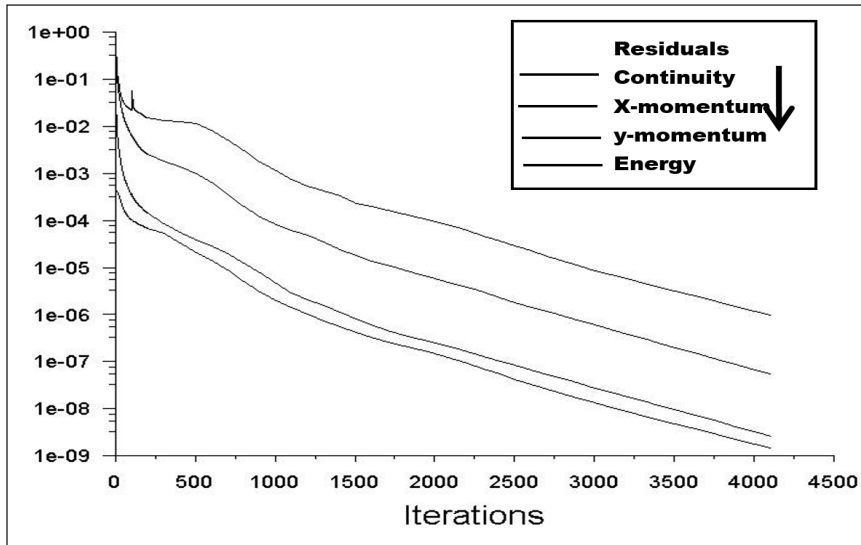


Figure 4. Error as a function of iteration number

VALIDATION

To validate the solution procedure, the numerical results obtained for both the streamlines and isotherms contours in an air-filled annular space between a heated inner concentric rotating cylinder and wavy surface outer cylinder were compared with results published by Yoo (1998). The comparison was done using the following parameters: $Ra = 10^5$, $Pr = 0.71$, at $l/D=2.5$, $Re=100, 300, 400$, and 600 , respectively. As can be seen in the Figure 5, close agreements were observed between the present results and those presented in Yoo (1998).

RESULTS AND DISCUSSION

The numerical investigations in this study were conducted under the following parameter ranges: amplitudes of the wavy surface ($L = 0, 1$ and 2), undulation numbers ($N = 5, 10$ and 15), Re ($Re = 0, 10, 100, 200, 400$ and 600) and Ra ($Ra = 10^3, 10^4$ and 10^5). Numerous results could be drawn from the output of ANSYS Fluent version 16.1 (ANSYS, 2014), such as pressure, flow trace, velocity vectors and streamline and isotherm contours. However, given the space limitation, only the results of the streamline and isotherm contours are shown in Figures 6(a–b) to 8(a–b). In addition, the heat transfer rate along the hot surface of the circular cylinder is expressed by local and average Nu , as shown in Figures 9(a–c) and 10.

Flow Structure and Thermal Fields

The flow structure and thermal fields were visualised using streamlines and isotherms, respectively. The streamline and isotherm patterns in Figures 6(a) and 6(b) demonstrated the effects of the amplitudes of the wavy surface, undulation numbers and Re on the flow

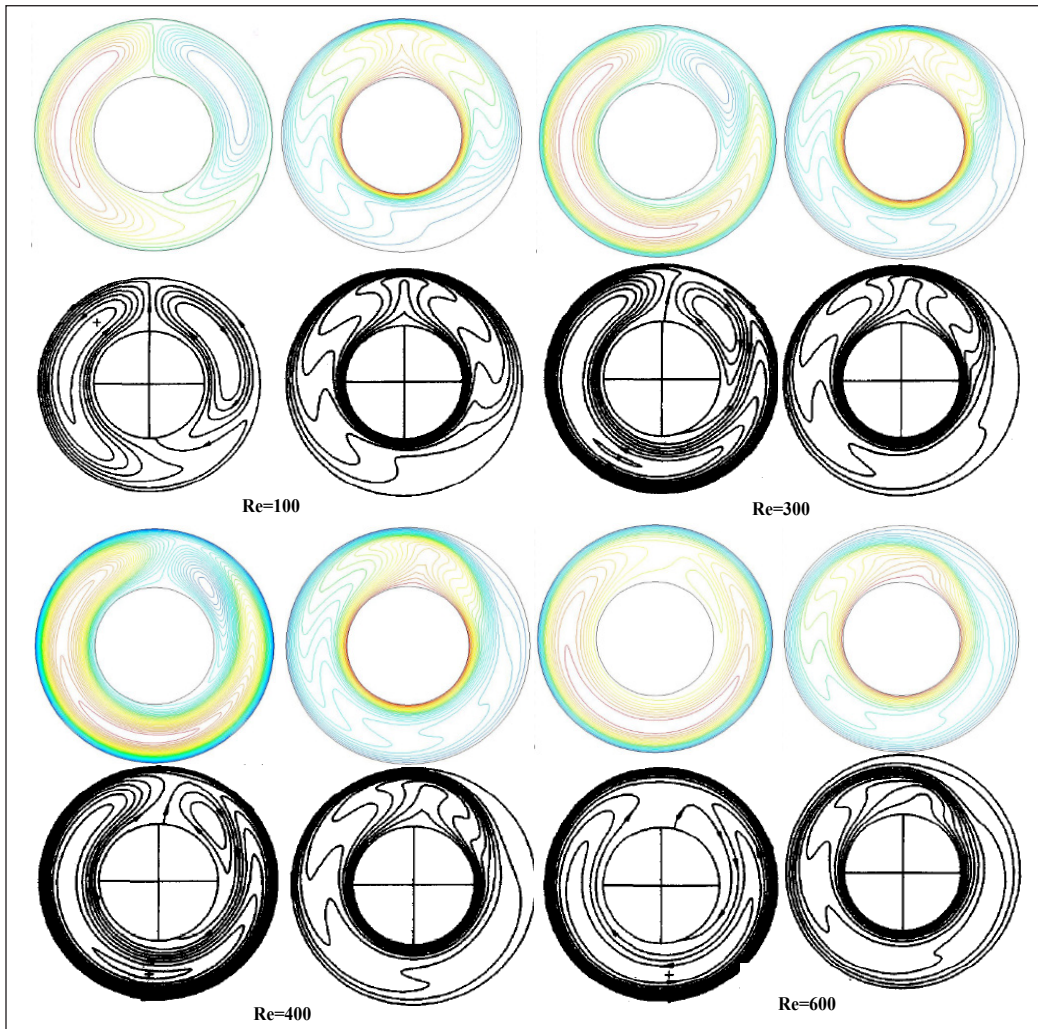


Figure 5. Comparison of streamline, isothermal line and heat transfer for present study and results of Yoo (1998) for $I/D=2.5$, $Pr=0.71$, $Ra=10^5$, $Re=100, 300, 400, \text{ and } 600$, respectively

structure and thermal fields for a fixed Ra of 10^3 . When the flow was at a low Ra of 10^3 and Re was equal to 0, the fluid motion inside the annulus was weak. The conduction or diffusion mode dominated the heat transfer between the hot and cold cylinders. In each selected case, the streamlines showed two rotating symmetric eddies; i.e. one on the right hand and the other on the left hand of the annular gap. These eddies were compressed and changed in the inner vortices inside each eddy possibly due to the wavy surface of the outer cylinder. Meanwhile, the isotherms were crowded around the hot inner cylinder and form parallel rings around the cylinder surface. Moreover, the contours of the streamlines and isotherms were somewhat systematic for those corresponding to $Re = 10$. As the value of Re increased to 100, the rotational speed of the inner cylinder led to a large change in the

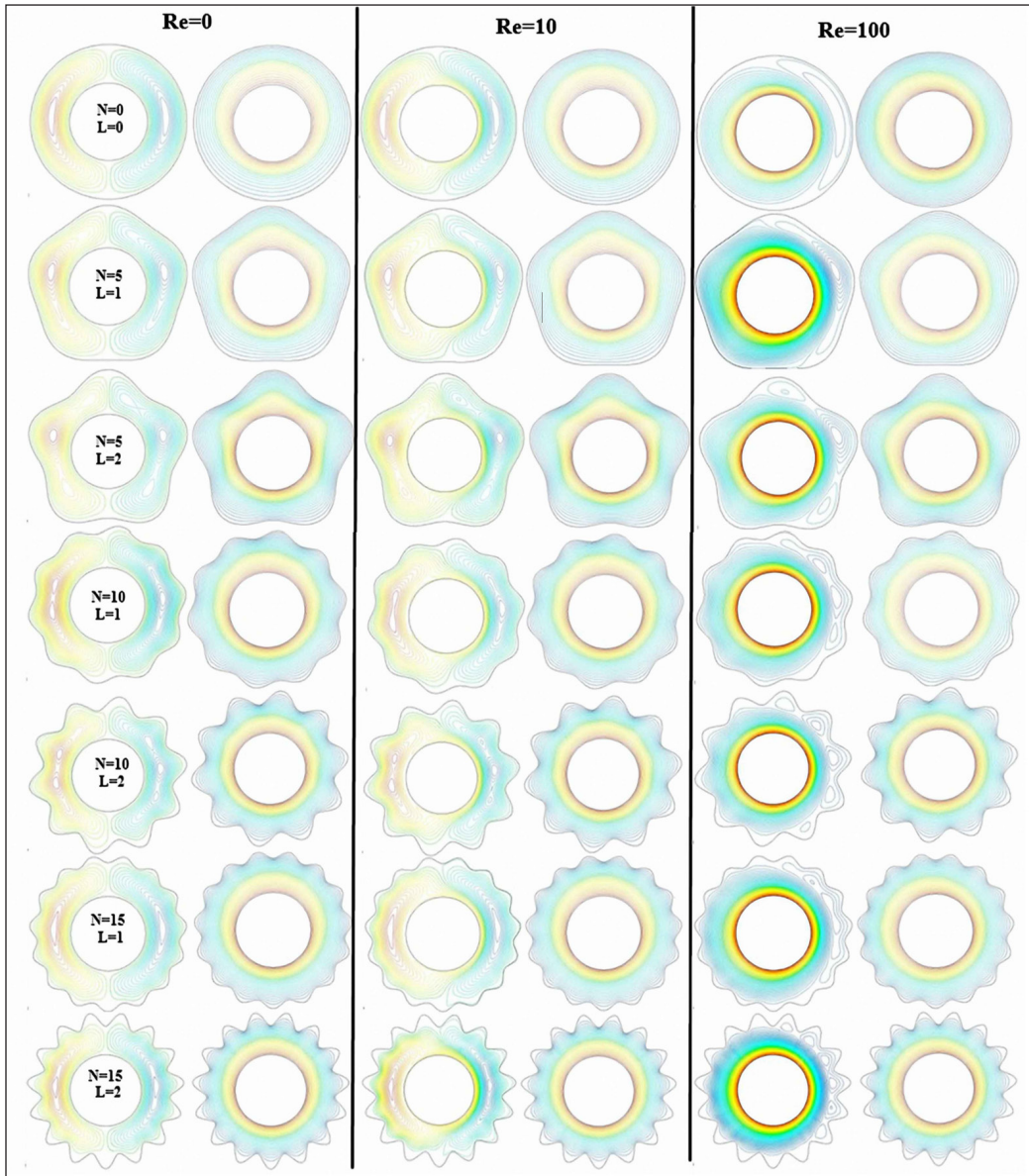


Figure 6a. Streamlines on left, Isothermal lines on right for Different Numbers of sinusoidal (N), amplitude (L) and Reynolds Number (Re=0,10,100) at $Ra=10^3$

flow field; hence, the streamlines were remarkably dense around the inner cylinder, and the two rotating eddies were progressively compressed to a single longitudinal eddy in the vicinity of the right side of the annulus gap case ($N = 0, L = 0$). In the other cases, the eddy was pushed to the wavy surface of the outer cylinder due to the centrifugal force and spread to the number of cells (i.e. three vortex cells for case $[N = 5, L = 2]$; five vortex cells for case $[N = 10, L = 2]$; and six vortex cells for case $[N = 15, L = 2]$).

The isotherm contours were similar to those of the previous values of Re . The effect of the rotation appeared to be strong such that the small eddies gradually disappeared with an increase in the Re to 200. This condition tends to enhance the influence of the flow induced by forced convection. When Re was increased from 400 to 600, the forced convection dominates the heat transfer and fluid flow. Consequently, the streamlines became concentric rings around the heated cylinder for each case. Conversely, the streamlines disappeared at the outer surface of the cylinder, where the effects of the cylinder rotation were weak. Meanwhile, the isotherms became more evenly distributed between the two cylinders as Re increased.

Figures 7(a) and 7(b) present the effects of the amplitudes of the wavy surface, undulation numbers and Re on the streamlines and isotherms at $Ra = 10^4$. This Ra value caused an increase in the buoyancy forces inside the annulus gap. For small values of Re (i.e. 0–10), the streamline contours exhibited two rotating eddies, i.e. developing in the right and left halves of the annulus gap. Furthermore, the rising hot fluid separated at the top of the inner cylinder to form a thermal plume (i.e. near $\theta = 90^\circ$). This phenomenon indicates that the inner thermal boundary layer begins to separate from the inner cylinder before reaching the top of the annulus. However, at ($N = 10, L = 2$), two small plumes appeared (i.e. nearly $\theta \approx 45^\circ$ and $\theta \approx 125^\circ$) in place of the usual single big plume. The two plumes yielded two secondary vortices over the upper portion of the annulus because of the increasing values of the wave amplitude. These vortices increased the heat transfer rates between the two cylinders. When Re further increased to 100, the effects of the rotation and the buoyancy appeared. The interaction between the two effects is called mixed convection. In the right part of the annulus, the forced and natural convection flows were combined because they were in the same anti-clockwise direction, but they were opposite in the left part. Therefore, the right cells seemed stronger than the left, thereby leading to the pushing of the cells in the anti-clockwise direction. Consequently, the pair of counter-rotating vortices, as presented in case ($N = 10, L = 2$), merged with the two main eddies. Then, the isotherms were strongly influenced by the rotation of the cylinder; thus, the thermal plume at the top of the inner cylinder was tilted in the direction of the cylinder rotation (i.e. nearly $\theta = 120^\circ$ for all cases). The patterns of the streamlines and isotherms when $Re = 200$ were predicted to be the same as those when $Re = 100$. With a further increase in Re from 400 to 600, the strength of the forced flow increasingly elevates. The thermal plume is progressively tilted at the top the inner cylinder towards the flow direction.

The streamline and isotherm contours are presented in Figures 8(a) and 8(b); these contours are for the same conditions as in Figures 7(a) and 7(b) but at $Ra = 10^5$. When Ra rose to 10^5 , the circulation effect of the eddies increased and the buoyancy force became the dominant mechanism that drove the convection of the fluid. The effect of the forced flow vanished when $Re = 0$. The fluid motion remained in the region of the natural

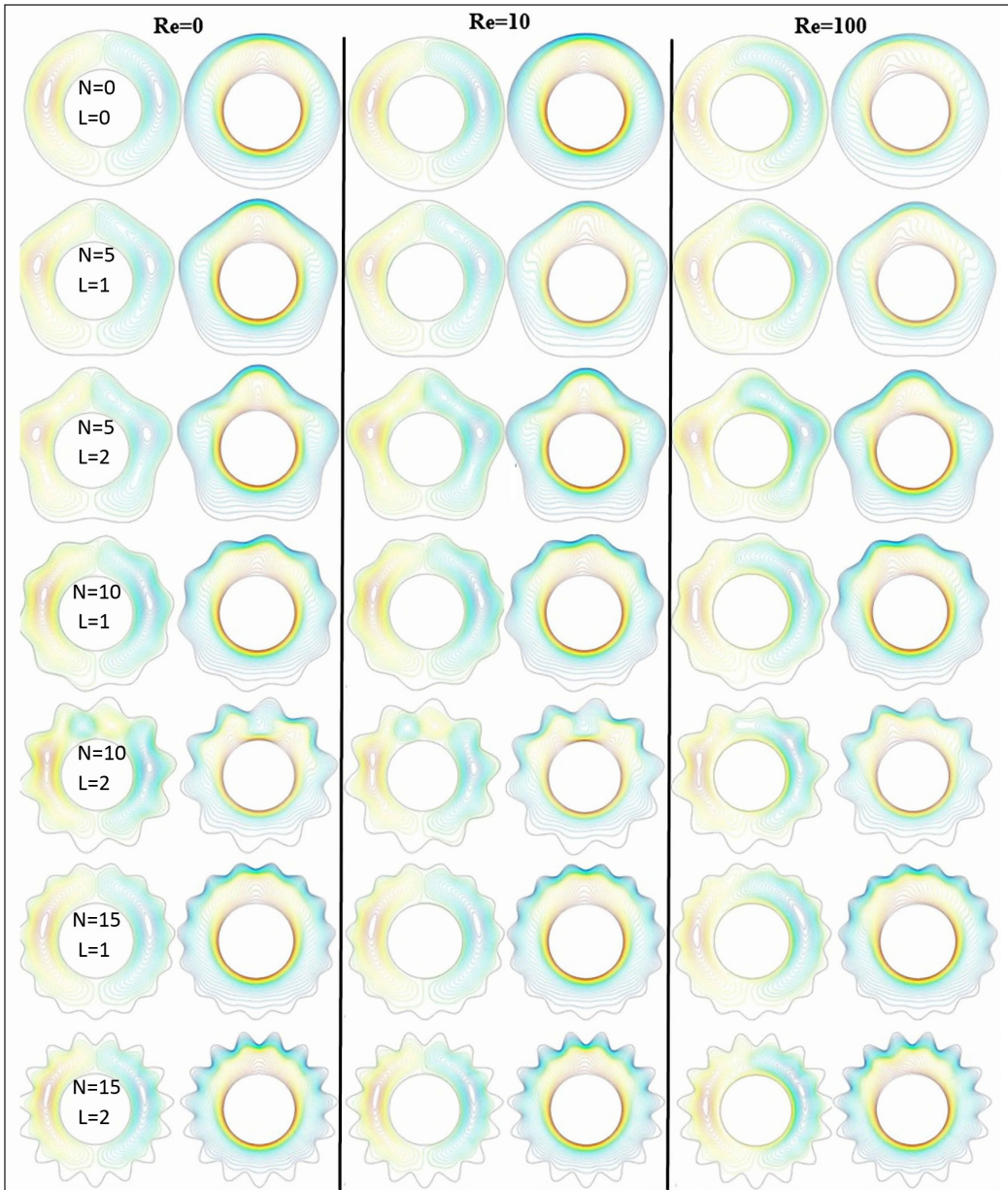


Figure 7a. Streamlines on left, Isothermal lines on right for Different Numbers of sinusoidal (N), amplitude (L) and Reynolds Number (Re) at $Ra=10^4$

convection, thus causing the formation of the two eddies in each flow pattern. However, the two eddies further rose upwards from the bottom half to the upper half inside the annulus gap due to the buoyancy effect. The flow was generated primarily due to the temperature gradient. As the temperature gradient developed with the increasing Ra , the shape of the isotherms moves upwards to form a thermal plume at the upper part of the annulus (i.e.

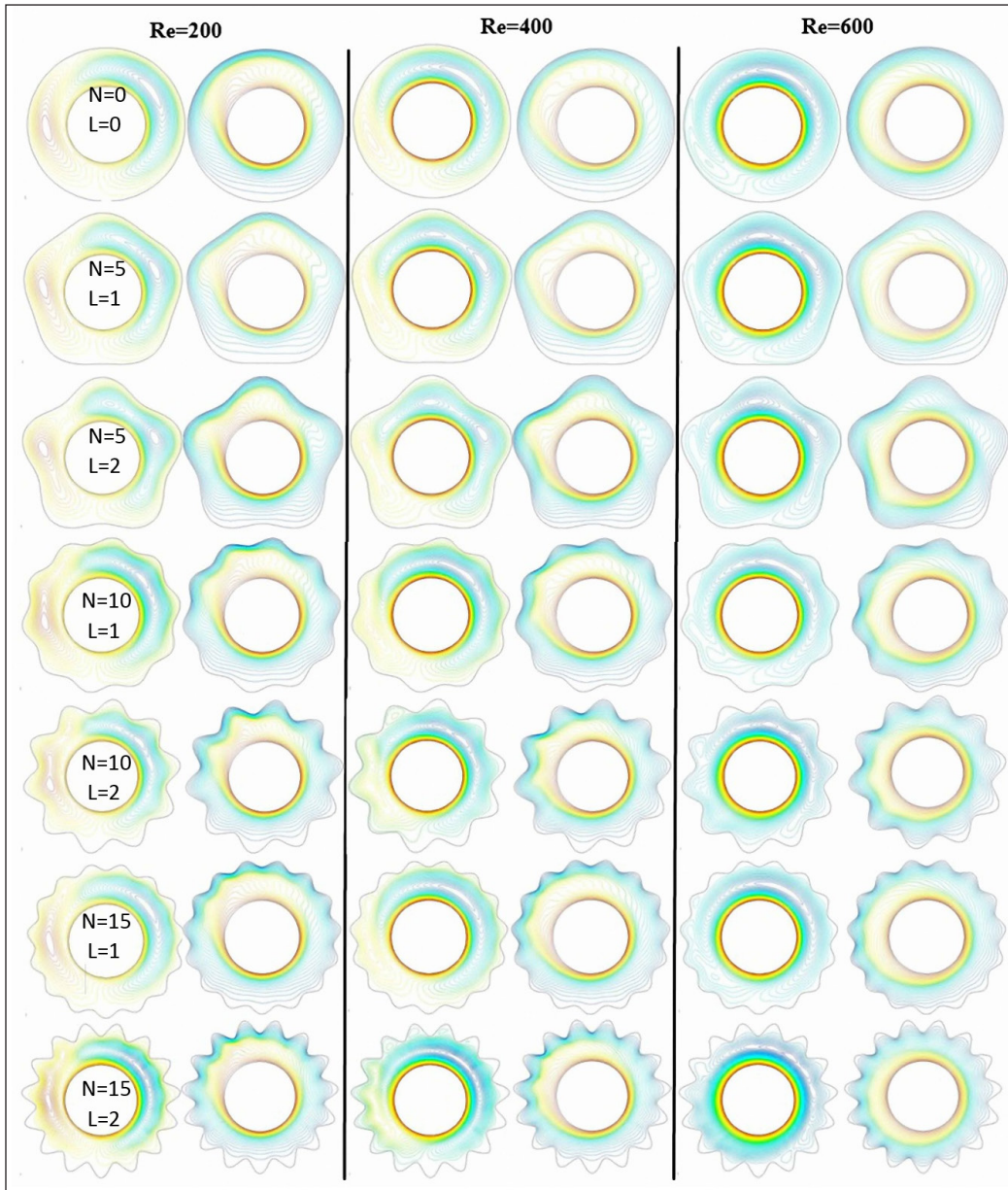


Figure 7b. Streamlines on left, Isothermal lines on right for Different Numbers of sinusoidal (N), amplitude (L) and Reynolds Number ($Re=200,400,600$) at $Ra=10^4$

nearly $\theta \approx 90^\circ$). However, at $(N = 15, L = 2)$, two thermal plumes developed around the angles $\theta \approx 45^\circ$ and $\theta \approx 120^\circ$ over the inner cylinder due to flow separation. In this case, two secondary vortices formed in the presence of the two eddies developing at the upper part of inner cylinder, thereby resulting in a large change in the streamline contour. These vortices produced two thermal plumes that rose to impinge the upper part of the outer

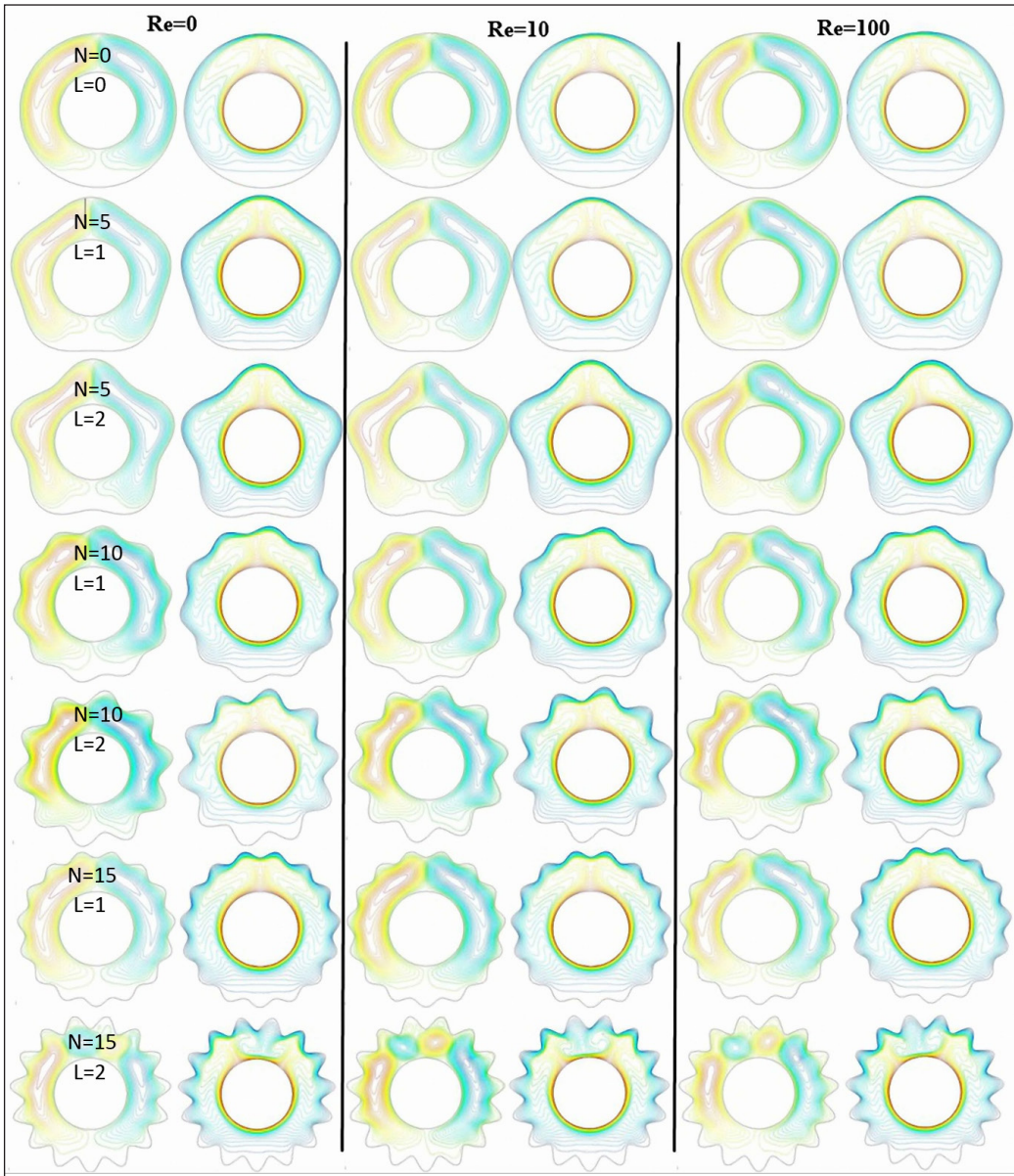


Figure 8a. Streamlines on left, Isothermal lines on right for Different Numbers of sinusoidal (N), amplitude (L) and Reynolds Number (Re=0,10, 100) at $Ra=10^5$

cylinder. Consequently, the impingement of the plume on the top of the outer cylinder led to the development of a thin thermal boundary layer, thus enabling high heat transfer due to natural convection. A type of symmetry was evident in the patterns of the streamlines and isotherms; this symmetry was similar to that when $Re = 10$. As Re increased to 100, the effect of the forced flow appeared. The eddy adjacent to the right-hand side of the inner cylinder started to move upwards. Conversely, the eddy on the left-hand side of the

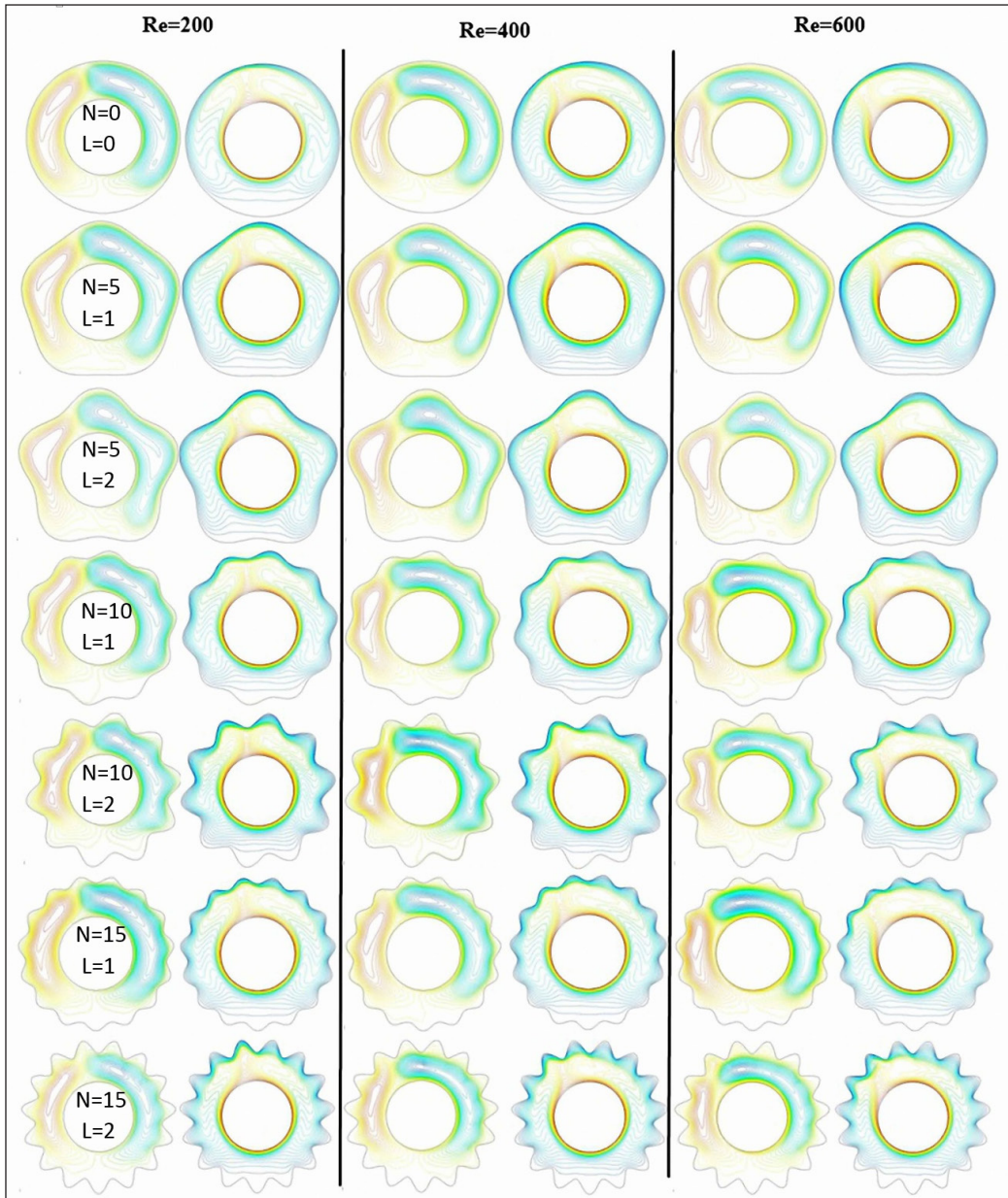


Figure 8b. Streamlines on left, Isothermal lines on right for Different Numbers of sinusoidal (N), amplitude (L) and Reynolds Number (Re=200,400,600) at $Ra=10^5$

inner cylinder was pulled downwards due to the viscous inner cylinder rotation. Thus, the isotherm patterns depicted that the thermal plume was slanted in the same direction as the rotating cylinder (i.e. nearly $\theta \approx 100^\circ$ for all cases). As Re was increased to 200, the contours of the streamlines and isotherms were shifted continuously towards the rotation of the inner cylinder (i.e. nearly $\theta \approx 115^\circ$ for all cases). In case (N = 15, L = 2), the two small

vortices at the top of the inner cylinder disappeared when Re increased to 200. When Re increased from 400 to 600, the shapes of the streamline and isotherm contours in all cases became slightly similar to those at $Re = 200$, but the thermal plume was slanted constantly in the same direction as the rotating cylinder with increasing Re (i.e. nearly $\theta \approx 135^\circ$ for $Re = 400$ and $\theta \approx 160^\circ$ for $Re = 600$).

Heat Transfer and Nu

Table 3 illustrates good agreement between the model result and reported result of Yoo (1998).

Table 3
Comparison of the average Nu between the present and Yoo (1998) results ($Re=0, Pr=0.71, l/D=2.5$)

Ra	Average Nu		
	Present study	Yoo(1998)	Deviation(%)
10^3	0.38189	0.392	1.01
10^4	0.67331	0.737	6.39
10^5	1.20832	1.2601	5.178

Figures 9(a–c) plot the distributions of local Nu values along the hot surface of the inner cylinder for different amplitudes of the wavy surface, undulation numbers and Re at $Ra = 10^3, 10^4$ and 10^5 . When the cylinder was stationary (i.e. $Re = 0$), the maximum value of the local Nu occurred around the bottom of the cylinder, existing in the vicinity of $\theta \approx 270^\circ$ for $Ra = 10^3$ and 10^4 . Meanwhile, it occurred at the two places between 210° and 315° at $Ra = 10^5$. In addition, the minimum value of the local Nu was obtained at the top surface of the inner cylinder (i.e. $\theta \approx 90^\circ$). However, two special cases occurred (i.e. $N = 10, L = 2$ at $Ra = 10^4$ and $N = 15, L = 2$ at $Ra = 10^5$) when a secondary flow was developed at the upper part of the inner cylinder such that the sudden increase in the local heat transfer manifested near the top of the inner cylinder (i.e. $\theta \approx 90^\circ$). In the same figure, the difference between the Nu_{max} and Nu_{min} values increased with the increasing Ra . When the inner cylinder was rotated at $Re = 10$, the maximum and minimum local Nu values were unaffected due to the small velocity of the inner cylinder. When Re increased to 100, the maximum and minimum values of the local Nu migrated along the rotational direction of the inner cylinder. The variation in the Nu curves became increasingly divergent at $Ra = 10^3$ when Re increased to 200 and was remarkably small when Ra equaled 10^4 and 10^5 . The sinusoidal distributions of the Nu curves became evident at $Ra = 10^3$ and were suppressed by an increase in the values of Re from 400 to 600. Therefore, the lines of the local Nu curves in this Re range strongly depended on the wavy surface of the outer cylinder and thus appearing to be wavy also. This behaviour disappeared at high Ra values (10^4 and 10^5) due to the boundary layer separation.

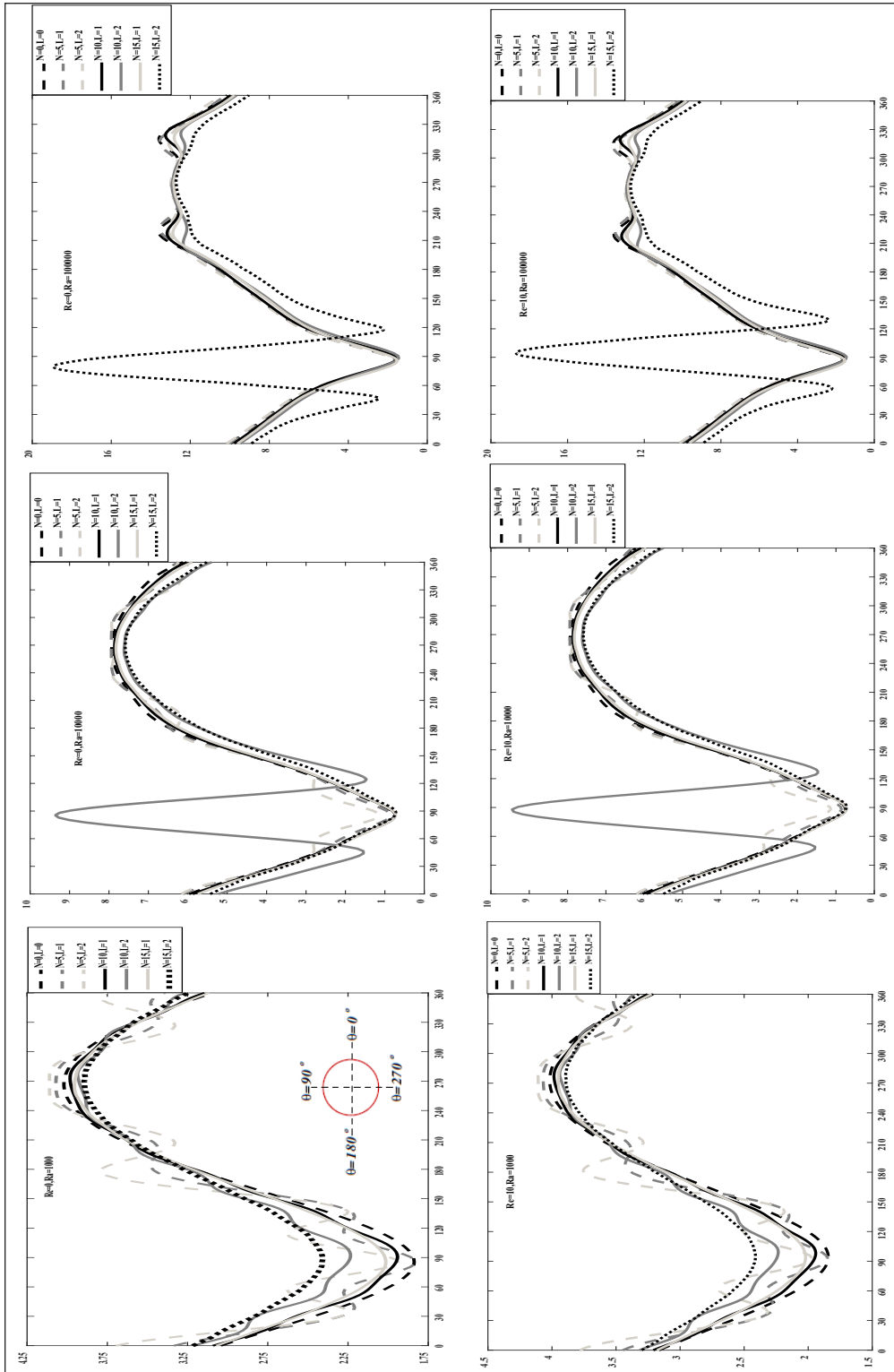


Figure 9a. Local Nusselt Number (y-axis) versus the inner cylinder surface (x-axis) at $Re=0$, and 10 for different $Ra=10^3$, 10^4 and 10^5 , respectively

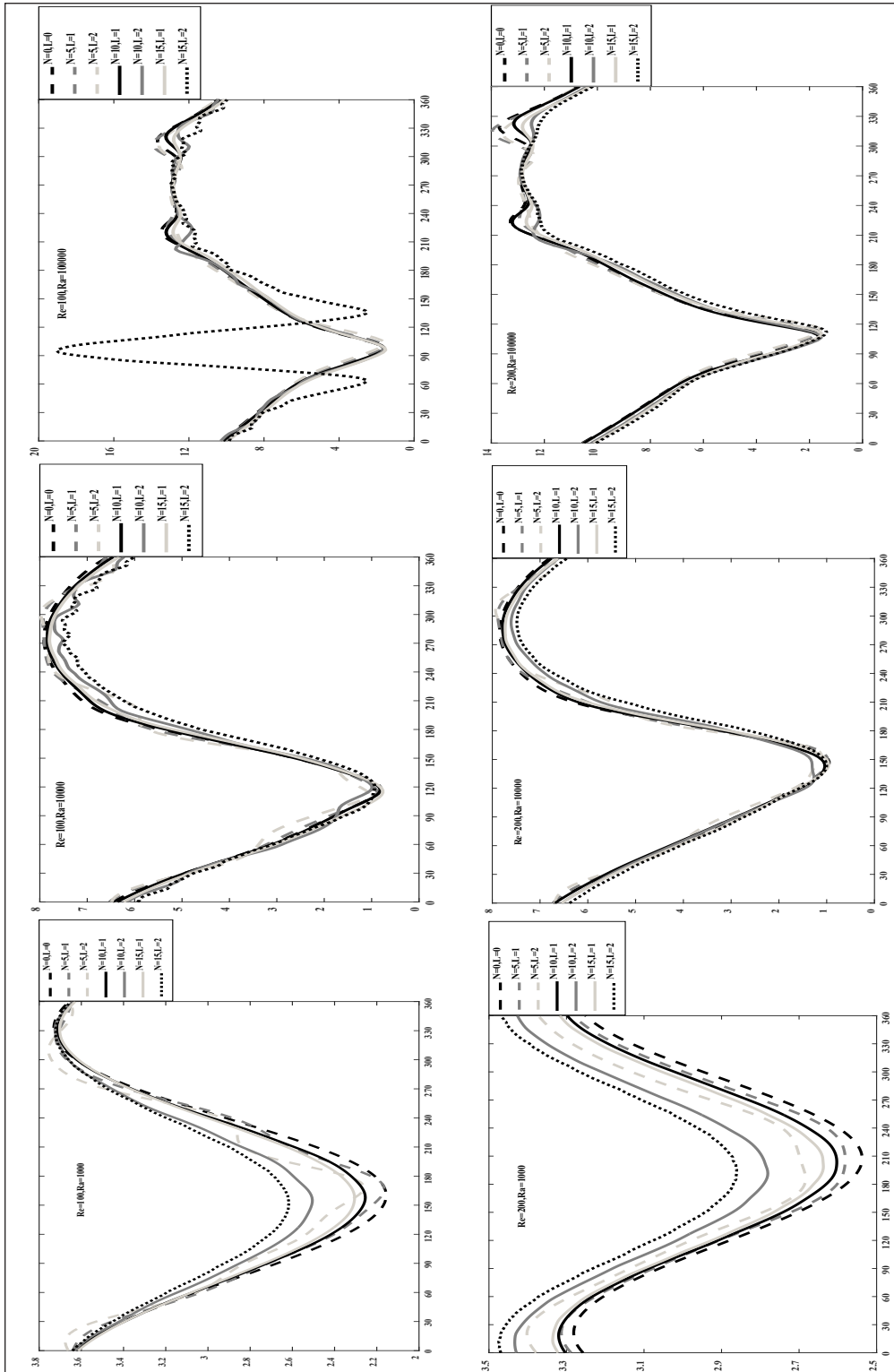


Figure 9b. Local Nusselt Number (y-axis) versus the inner cylinder surface (x-axis) at $Re=100, 200$ for different $Ra=10^3, 10^4$ and 10^5 , respectively

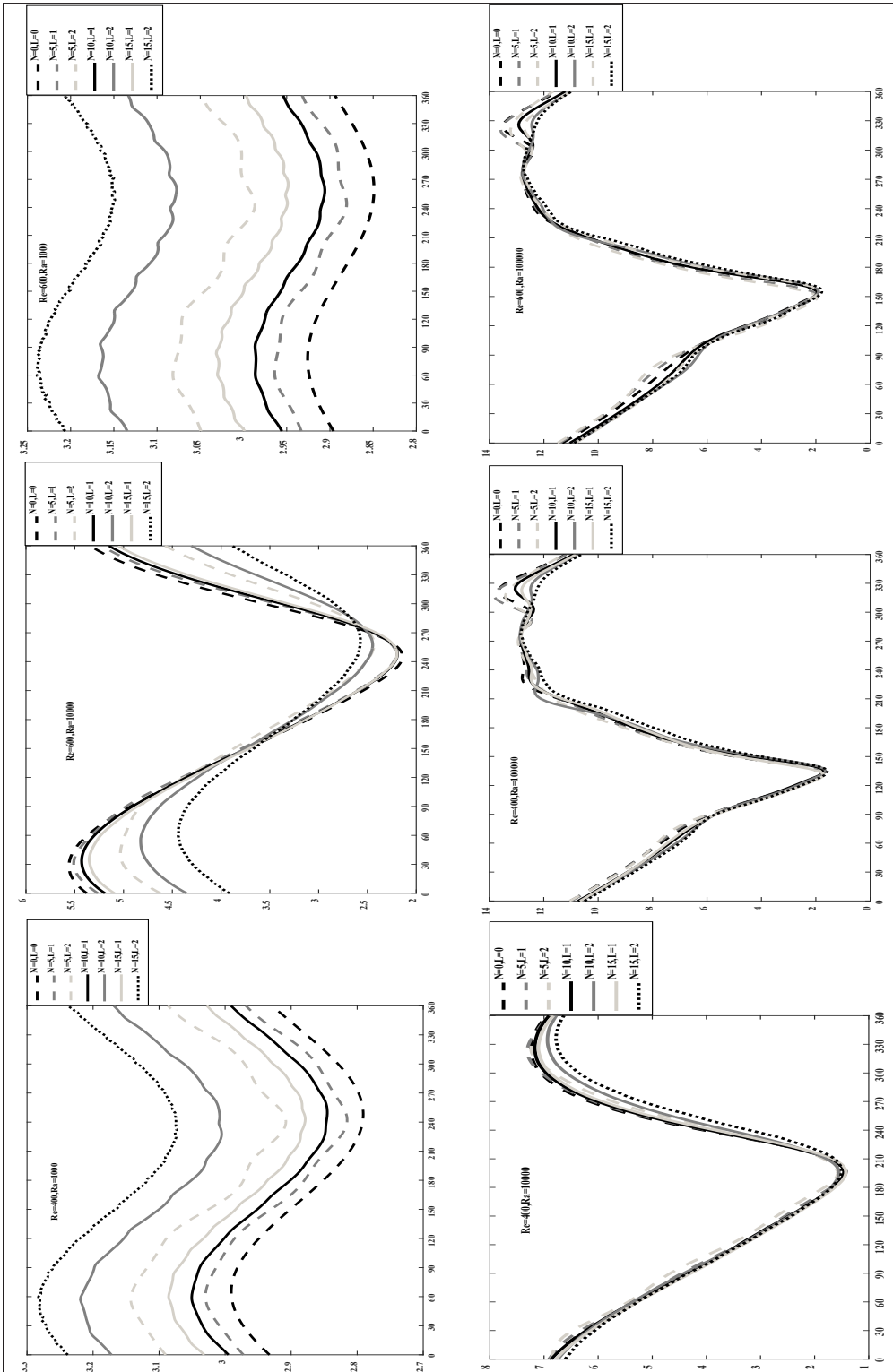


Figure 9c. Local Nusselt Number (y-axis) versus the inner cylinder surface (x-axis) at $Re=400$, and 600 for different $Ra=10^3$, 10^4 and 10^5 , respectively.

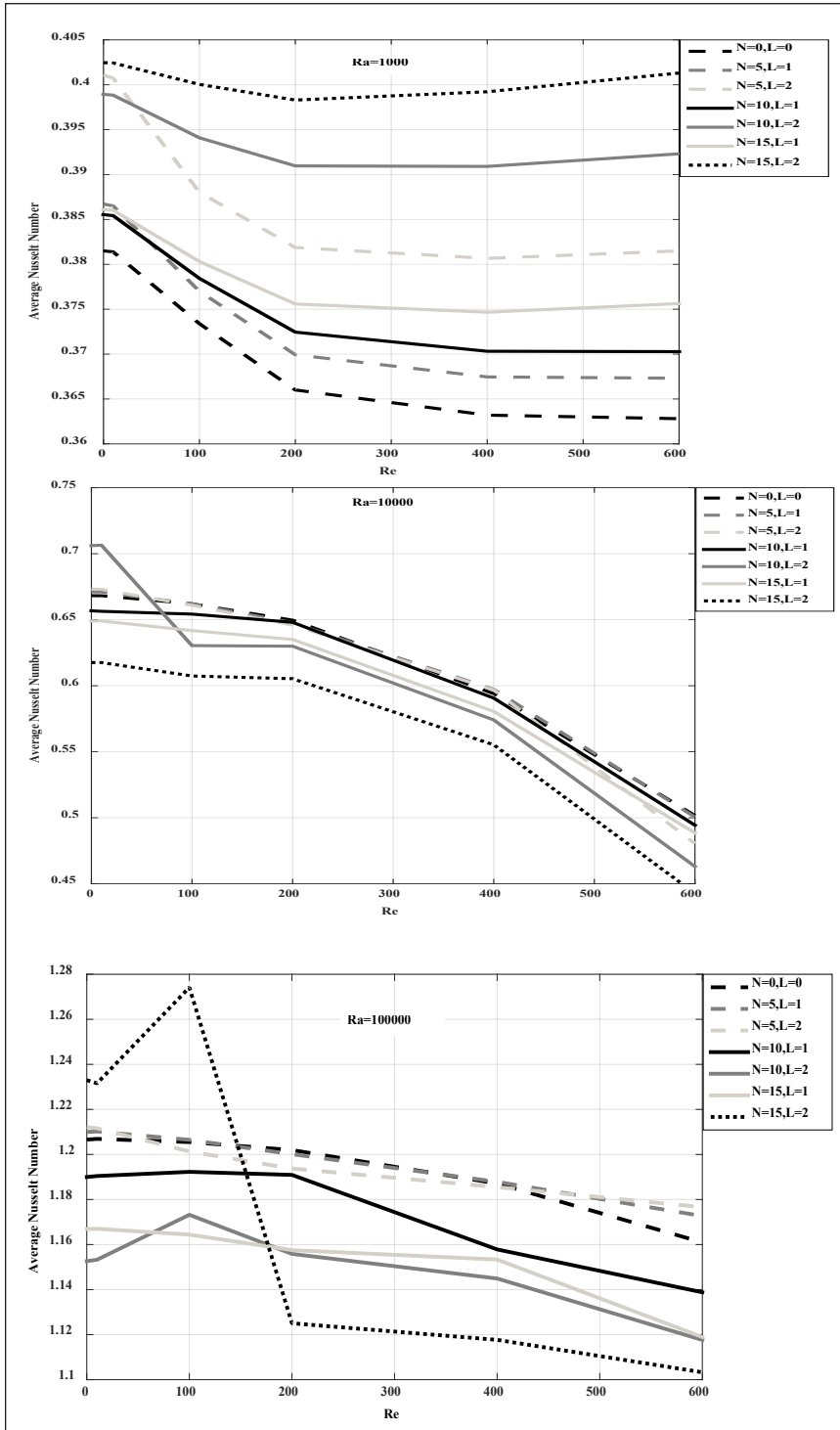


Figure 10. Average Nusselt Number as a function of amplitudes of wavy surface, undulation numbers and Reynolds numbers for $Ra= 10^3$, 10^4 and 10^5 , respectively.

Figure 10 reveals the average Nu as a function of Re, amplitudes of the wavy surface and undulation numbers for different Ra values ($Ra = 10^3$, 10^4 and 10^5). At $Ra = 10^3$, a rapid decrease in the average Nu was observed for all cases at low Re values (0 to approximately 200). However, beyond this Re range, the average Nu was gradually decreased except when the amplitudes of the wavy surface increased to two ($N = 5$, $N = 10$ and $N = 15$ for $L = 2$) possibly due to the periodic channelling offered by the wavy surfaces of the outer cylinder, which led to increases in the heat transfer rate and the average Nu by approximately 7.3%. With an increase in Ra to 10^4 , the average Nu decreased in tandem as the Re increased by approximately 2.4%. At a high Ra ($Ra = 10^5$), the average Nu decreased when Re increased except at ($N = 10$, $L = 2$) and ($N = 15$, $L = 2$), where the average Nu increased when Re ranged between 10 and 200 due to the rising wave amplitude.

CONCLUSIONS

The present numerical study is conducted for the mixed convection in the annular space between two concentric cylinders. The heated circular inner cylinder rotates with constant angular velocity, whereas the cold outer cylinder with a sinusoidal surface is stationary. Results show that the streamline and isotherm contours were affected by the changes in the sinusoidal surface parameters of the outer cylinder, such as amplitudes of the wavy surface and undulation numbers for different values of Re and Ra. The conclusions are as follows.

1. The isotherms and streamlines primarily depend on Ra, amplitudes of the wavy surface and undulation numbers.
2. The heat transfer from the inner cylinder increases with a rise in the surface amplitudes and undulation numbers with a fixed Re.
3. In each case, the average Nu on the surface of the inner cylinder increases with the rise of the thermal Ra and decreases throughout the flow if the rotational Re is increased.
4. The average Nu increases when the surface amplitudes and undulation numbers increase by approximately 7.3% for $Ra = 10^3$; it decreases as the surface amplitude and undulation numbers simultaneously increase by approximately 2.4% for $Ra = 10^4$ and 10^5 .

ACKNOWLEDGEMENT

Authors wish to thank the University of Babylon for their help and technical support.

REFERENCES

- Alam, M., Kamruzzaman, Ahsan, F., & Hasan, M. N. (2016). Mixed convection heat transfer inside a differentially heated square enclosure in presence of a rotating heat conducting cylinder. *AIP Conference Proceedings*, 1754(1), 1-8.

- Alsabery, A. I., Tayebi, T., Chamkha, A. J., & Hashim, I. (2018). Effect of rotating solid cylinder on entropy generation and convective heat transfer in a wavy porous cavity heated from below. *International Communications in Heat and Mass Transfer*, 95, 197-209.
- ANSYS. (2014). *ANSYS fluent theory guide (Release 16.1)*. Canonsburg, Pennsylvania: ANSYS, Inc.
- Bande, Y. M., & Mariah, N. A. (2014). Flat plate solar collectors and applications : a review. *Journal of Science and Technology*, 22(2), 365-385.
- Boyd, R. D. (1984). Interferometric study of natural convection heat transfer in a horizontal annulus with irregular boundaries. *Nuclear Engineering and Design*, 83(1), 105-112.
- Chamkha, A. J., Hussain, S. H., & Abd-Amer, Q. R. (2011). Mixed convection heat transfer of air inside a square vented cavity with a heated horizontal square cylinder. *Numerical Heat Transfer; Part A: Applications*, 59(1), 58-79.
- El-Shaarawi, M., & Sarhan, A. (1982). Combined forced-free laminar convection in the entry region of a vertical annulus with a rotating inner cylinder. *International Journal of Heat and Mass Transfer*, 25(2), 175-186.
- Hussain, S. H., & Abd-Amer, Q. R. (2011). Mixed convection heat transfer flow of air inside a sinusoidal corrugated cavity with a heat-conducting horizontal circular cylinder. *Journal of Enhanced Heat Transfer*, 18(5), 433-447.
- Lee, T. S. (1992). Numerical computation of fluid convection with air enclosed between the annuli of eccentric heated horizontal rotational cylinder. *Computers Fluids*, 21(3), 355-368.
- Mohammed, A. (2007). Mixed convection in the entry region of a vertical annulus with a constant temperature rotating inner cylinder. *Engineering and Technology*, 25(1), 78-96.
- Mozayyeni, H. R., & Rahimi, A. B. (2011). Mixed convection in cylindrical annulus with rotating outer cylinder and constant magnetic field with an effect in the radial direction. *Scientia Iranica*, 19(1), 91-105.
- Rajamohan, G., Narayanaswamy, R., & Kumar, P. (2015). Experimental study on mixed convection heat transfer in a square duct with varying: inclination angles. *Journal of Science and Technology*, 23(1), 141-151.
- Sheikholeslami, M., Gorji-Bandpy, M., Ganji, D. D., Soleimani, S., & Seyyedi, S. M. (2012). Natural convection of nanofluids in an enclosure between a circular and a sinusoidal cylinder in the presence of magnetic field. *International Communications in Heat and Mass Transfer*, 39(9), 1435-1443.
- Sheikholeslami, M., Gorji-Bandpy, M., Pop, I., & Soleimani, S. (2013). Numerical study of natural convection between a circular enclosure and a sinusoidal cylinder using control volume based finite element method. *International Journal of Thermal Sciences*, 72, 147-158.
- Sheikholeslami, M., Gorji-Bandpy, M., Ganji, D. D., & Soleimani, S. (2014). MHD natural convection in a nanofluid filled inclined enclosure with sinusoidal wall using CVFEM. *Neural Computing and Applications*, 24(3-4), 873-882.
- Shekar, B. C., Vasseur, P., Robillard, L., & Nguyen, T. H. (1984). Natural convection in a heat generating fluid bounded by two horizontal concentric cylinders. *The Canadian Journal of Chemical Engineering*, 62(4), 482-489.

- Shih, Y. C., Khodadadi, J. M., & Weng, K. H. (2009). Periodic fluid flow and heat transfer in a square cavity due to an insulated or isothermal rotating cylinder. *Journal of Heat Transfer*, 131(11), 1-11.
- Wang, Y. F., Xu, X., Tian, T., Fan, L. W., Wang, W. L., & Yu, Z. T. (2015). Laminar mixed convection heat transfer of SiC-EG nanofluids in a triangular enclosure with a rotating inner cylinder: simulations based on the measured thermal conductivity and viscosity. *Journal of Zhejiang University-SCIENCE A*, 16(6), 478-490.
- Xu, X., Yu, Z., Hu, Y., Fan, L., & Cen, K. (2010). A numerical study of laminar natural convective heat transfer around a horizontal cylinder inside a concentric air-filled triangular enclosure. *International Journal of Heat and Mass Transfer*, 53(1-3), 345-355.
- Xu, X., Sun, G., Yu, Z., Hu, Y., Fan, L., & Cen, K. (2009). Numerical investigation of laminar natural convective heat transfer from a horizontal triangular cylinder to its concentric cylindrical enclosure. *International Journal of Heat and Mass Transfer*, 52(13-14), 3176-3186.
- Yoo, J. (1998). Mixed convection of air between two horizontal concentric cylinders with a cooled rotating outer cylinder. *International Journal of Heat and Mass Transfer*, 41(2), 293-302.
- Yuan, X., Tavakkoli, F., & Vafai, K. (2015). Analysis of natural convection in horizontal concentric annuli of varying inner shape. *Numerical Heat Transfer, Part A: Applications*, 68(11), 1155-1174.
- Yu, Z. T., Fan, L. W., Hu, Y. C., & Cen, K. F. (2010). Prandtl number dependence of laminar natural convection heat transfer in a horizontal cylindrical enclosure with an inner coaxial triangular cylinder. *International Journal of Heat and Mass Transfer*, 53(7-8), 1333-1340.

